JOURNAL OF GEOPHYSICAL RESEARCH, VOL. 106, NO. B10, PAGES 21,965–21,977, OCTOBER 10, 2001

Fluid inclusions in pseudotachylytes from the Nojima fault, Japan

Anne-Marie Boullier

Laboratoire de Géophysique Interne et Tectonophysique, CNRS, Université Joseph Fourier, Grenoble, France

Tomoyuki Ohtani, Koichiro Fujimoto, and Hisao Ito

Geological Survey of Japan, National Institute of Advanced Industrial Science and Technology, Tsukuba, Japan

Michel Dubois

Sédimetologie et Géodynamique, Université des Sciences et Techniques de Lille, Villeneuve d'Ascq, France

Abstract. Pseudotachylytes (i.e., rocks formed by frictional melting) have been observed in the Nojima fault that was penetrated by the Hirabayashi borehole drilled 1 year after the 1995 Hyogo-ken Nanbu (Kobe) earthquake. These rocks display millimeter-scale banding defined by different pseudotachylyte layers. The nature of unmolten crystal fragments (K-feldspar, albite, calcite, and/or quartz) allows us to infer a minimum melting temperature of 1200°C. The glass has a 8 ± 3% volatile content and a higher CaO content than that of the parent granodiorite, thus suggesting that pseudotachylyte formation occurred in an already altered, calcite-bearing and hydrated fault zone. Fluid inclusions have been observed in the glass and are filled with a dense low-salinity (4.3 ± 1.2 wt % eq. NaCl) CO_2-H_2O fluid characterized by steep isochoric curves. The intersection between the isochores and the measured 24°C/km geothermal gradient indicates a minimum 15 km depth for the pseudotachylyte formation. Such a depth suggests that an important uplift has brought the studied pseudotachylytes to their present position and that these pseudotachylytes are probably pre-Miocene in age. The calculated thermal evolution of a typical millimeter-scale pseudotachylyte layer indicates that cooling does not last more than a few seconds. This indicates that related seismic processes, such as deceleration of fault movement and healing of the fault, were both very rapid. The geometry and thermal budget of the millimeter-thick pseudotachylytes suggest that seismic events of magnitude 6 to 7 are responsible for their formation.

1. Introduction

Recordings on seismographs provide information on the location of the source and the focal mechanism, on the magnitude and duration of the slip event, and on the stress drop and radiated energy. The fault zone itself, however, is usually not accessible to observations needed to document its structure in relation to the rupture and to constrain the small-scale deformation mechanisms operating within the fault in relation to the seismic cycle. For example, the width of a fault zone is a crucial parameter for deducing the thermal budget during seismic slip [*Kanamori and Heaton*, 2000], and this parameter can only be approached by the observation of active faults.

The first opportunity to observe a recently ruptured fault was provided by the Geological Survey of Japan (GSJ) 1 year after the 1995 Hyogo-ken Nanbu (Kobe, Japan) earthquake. Several subvertical boreholes have been drilled which encounter the active Nojima fault and therefore provide the opportunity to study the physical and chemical properties of an active fault. In particular, pseudotachylytes have been recognized within the fault core in the GSJ borehole [*Fujimoto et al*., 1999; *Tanaka et al*., 2001]. Fluid inclusions have been observed for the first time in the pseudotachylytic glass. The aim of this paper is to describe the specific features of these pseudotachylytes, and especially the fluid inclusions, which could provide some information on the depth of formation of the frictional melt, on the characteristics of the slip events, and on their thermal budget during seismic rupture.

Paper number 2000JB000043.
0148-0227/01/2000JB000043$09.00

2. Geological Setting

The 1995 Hyogo-ken Nanbu earthquake (M_{JMA} = 7.2, M_W = 6.9) produced a 10.5-km-long surface break along the Nojima fault on the northwest coast of Awaji Island south of Kobe [*Awata and Mizuno*, 1997]. One year later, the Geological Survey of Japan drilled a 746.7-m-deep subvertical borehole which encountered the fault within a Cretaceous granodiorite and porphyry dikes between 623.1 and 625.3 m depth (Figure 1). Conventional logging (electrical resistivity and natural gamma radioactivity) and other logging tools, such as monopole and dipole sonic waveforms, microresistivity, and ultrasonic borehole televiewing, were used in order to allow a complete characterization of the borehole [*Ito et al*., 1999]. Cores were recovered corresponding to almost the entire depth interval from 150.2 to 746.7 m. The petrography, mineralogy (primary and alteration paragenesis), and structures

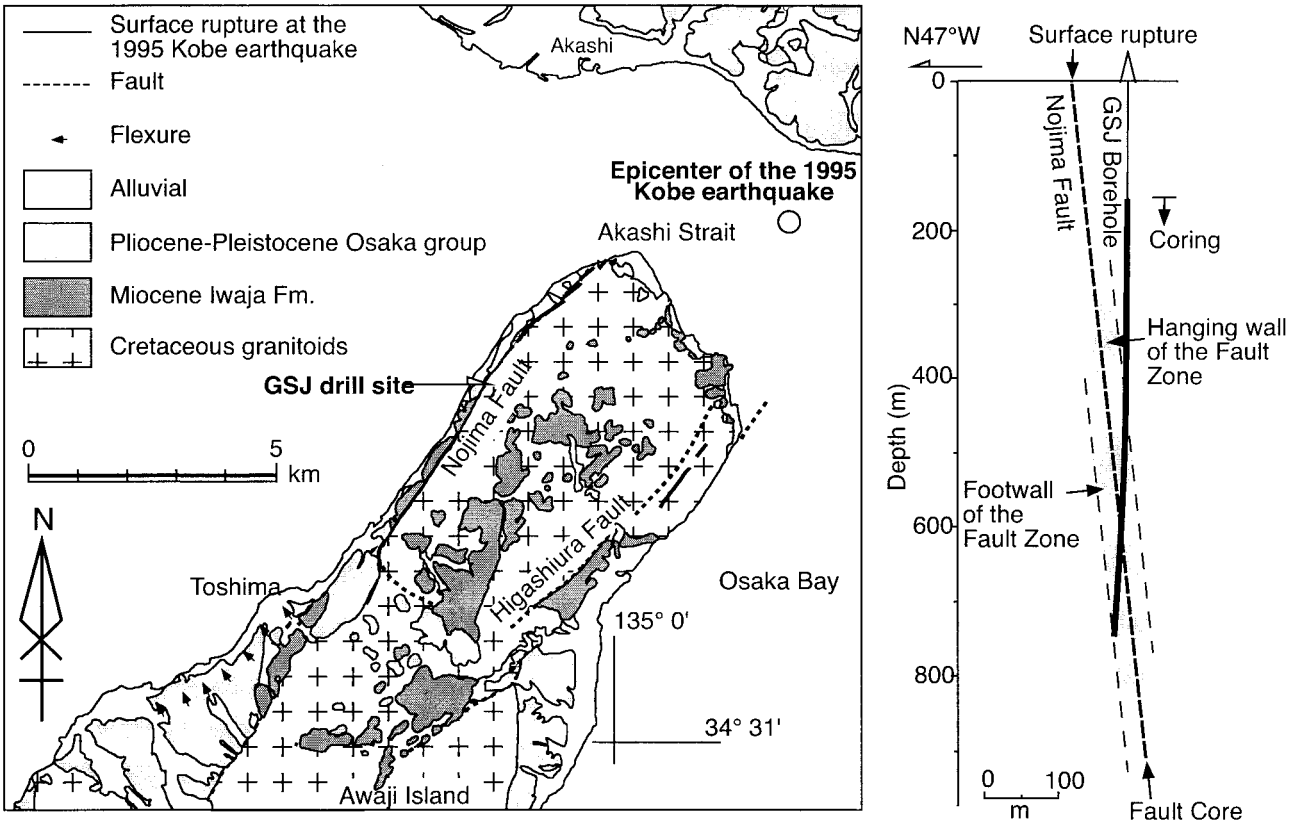

Figure 1. Generalized local geology of the northern part of the Awaji Island and location and orientation of the Hirabayashi GSJ borehole [after *Ohtani et al*., 2000].

along the whole drill core have been described by *Ito et al*. [1996], *Tanaka et al*. [1999, 2001], and *Ohtani et al*. [2000]. In the fault core itself (623.1–625.3 m depth), *Fujimoto et al*. [1999] describe different types of fault gouges on the basis of macroscopic and microscopic criteria and have recognized pseudotachylytes, i.e., fault rocks originated by frictional melting [*Sibson*, 1975; *Snoke et al*., 1998], within two narrow zones. This paper concerns such a pseudotachylyte situated at 624.59 m depth within the Nojima fault core and in which we have been able to recognize and characterize fluid inclusions.

3. Textures

Two thin sections perpendicular to the fault plane at 624.59 m depth have been studied; Figure 2 shows one vertically oriented thin section (parallel to the core axis) and one horizontally oriented thin section (perpendicular to the core axis). Both thin sections display a millimeter-thick dark gray or brown color banding. In the vertical thin section, minor subhorizontal or low-dip reverse fractures crosscut the steeply dipping foliation, indicating a shortening direction perpendicular to the fault plane, i.e., a horizontal shortening [see also *Ohtani et al*., 2000, Figure 5e]. These fractures are generally filled either by calcite or by laumontite. However, a layer of pseudotachylyte has been observed to be intruded along such fractures (white arrows in Figure 2), suggesting that these small faults were already active during the formation of the pseudotachylytes.

The millimetric layers of pseudotachylytes display slightly different color, various types and sizes of crystal fragments [*Magloughlin and Spray*, 1992] and are generally separated by thin layers of brecciated pseudotachylytes. Locally, a finely layered pseudotachylyte is folded and the fold hinges are boudinaged, disrupted, isolated, and embedded in a homogeneous glassy pseudotachylyte (Figure 3). Similar features have been observed by *Otsuki et al*. [1999] in pseudotachylytes outcropping on the Nojima fault surface break and have been interpreted by Otsuki et al. as older pseudotachylyte layers plastically deformed and reworked in a younger one. Rounded crystal fragments are present in the homogeneous glassy phase. They are <50 μm in diameter and are composed of quartz, calcite, albite, and K-feldspar. In some pseudotachylyte layers, only quartz fragments remain and display blurred contours (Figure 4). No microlites, graphite, sulfide droplets, or opaque blebs, such as those described by *Magloughlin* [1992], have been observed in the Nojima pseudotachylytes.

In some layers, abundant vesicles are easily observed in the glassy phase with scanning electron microscopy (SEM). When observed in transmitted light, these vesicles appear to be fluid inclusions which will be described in detail in section 5. The pseudotachylyte layers display various degrees of fracturing and brecciation. Ultracataclasites (or very fine grained fault gouges) may be juxtaposed against pseudotachylyte layers (Figure 5) and are composed of mineral (quartz, K-feldspar, carbonate, zeolite, and rare albite) and glassy pseudotachylyte fragments up to 100 μm in diameter occurring within a very fine grained matrix. These layers do not show any visible shear localization structures, as already demonstrated by *Otsuki et al*.

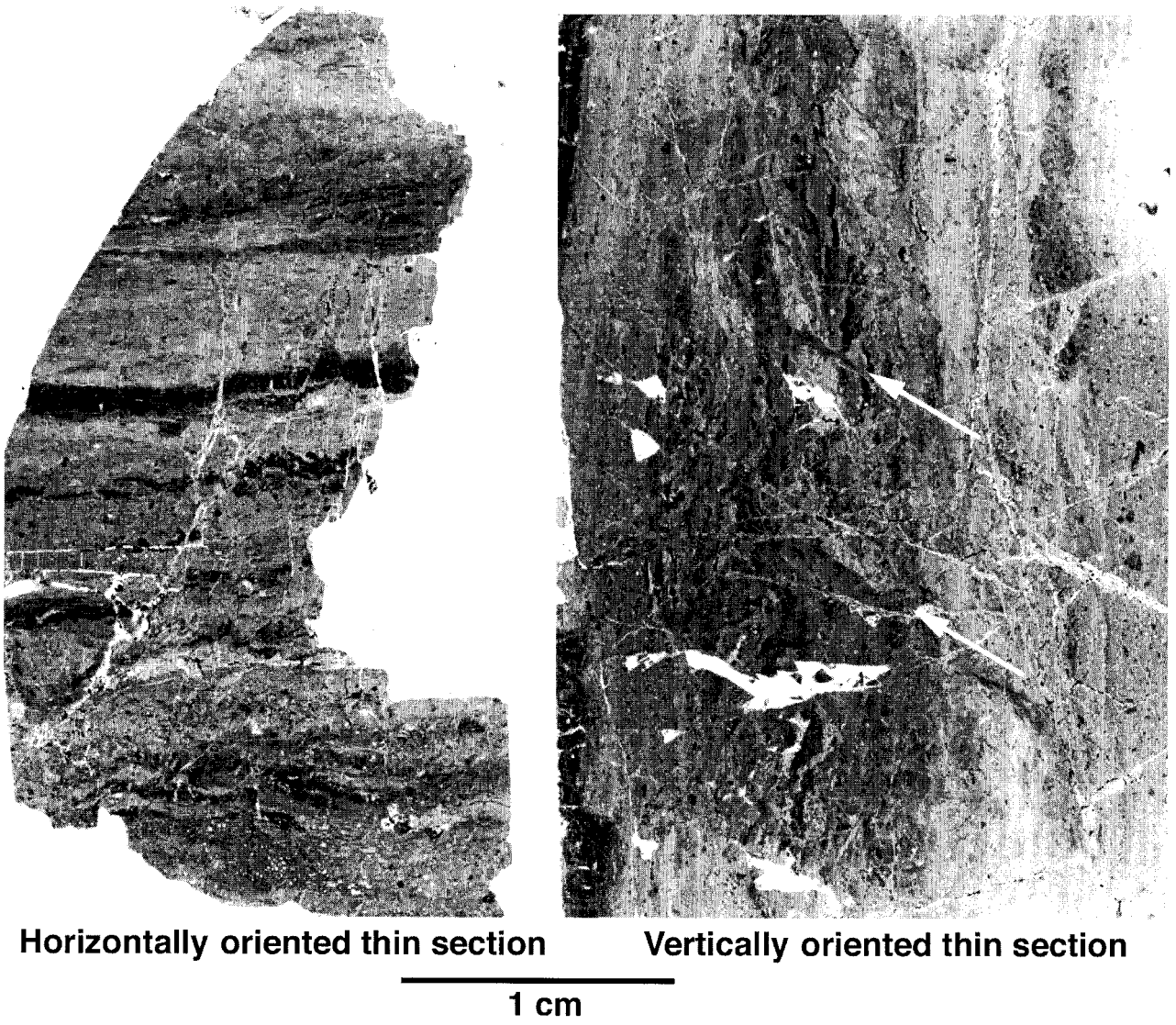

Figure 2. Numerical scans of the vertically and horizontally oriented thin sections of the 624.59 sample showing the millimeter-scale banding. On the vertically oriented thin section the layering is displaced by small conjugate fractures in which a pseudotachylyte layer is intruded (white arrows). These small faults indicate a shortening perpendicular to the main fault plane.

[1999]. The contact between the pseudotachylyte and ultracataclasite layers is sharp or slightly curved and roughly parallel to the layering. The fact that the fragments are larger in size and more variable in nature in the cataclasite than in the pseudotachylyte suggests that the latter postdates the cataclasite. However, a general rule could not be established, and *Otsuki et al*. [1999] describe conflicting crosscutting relationships between ultracataclasites and pseudotachylytes.

4. Composition of the Glass Phase

The composition of the glass phase has been determined with an electron microprobe (Cameca SX100, Montpellier University, France), operating at 20 kV, 10-nA beam current, and 20-s counting time. The results are reported in Table 1. The average total of all oxides is 92 ± 3%, and the significance of the 8% remaining difference may be discussed on the basis of the following points. Almost all major oxides except P_2O_5 have been measured in the granodiorite [*Tanaka et al*., 1999, 2001] and in the glass, and the P_2O_5 content in the granodiorite is only 0.11%. Using the above operating conditions, the relative uncertainty on oxide content, such as Na_2O, induced by element migration is <10% [*Reed*, 1996]. Concentrations of the minor elements analyzed by *Tanaka et al*. [1999, 2001] in the granodiorite do not exceed a total of 2000 ppm. Therefore the 8% remaining difference is inferred to represent mostly volatiles dissolved in the glass phase.

The content of dissolved volatiles decreases with increasing SiO_2 content of the glass (Figure 6a) and is lowest for points measured in the vicinity of incompletely molten quartz fragments (points 3 and 11, Table 1). The composition of the glass may be compared with that of the average composition of the undeformed granodiorite given by *Tanaka et al*. [1999, 2001] when recalculated without volatiles (Figure 6b). The SiO_2 and CaO contents are generally higher in the glass than in the granodiorite, whereas the reverse is true for K_2O, FeO, Na_2O, and MgO. The Al_2O_3 content is almost identical in both the

Figure 3. Microphotograph showing the layering and disrupted folds of an older pseudotachylyte layer embedded in a younger one. The long axes of the ellipsoidal fluid inclusions are indicated by the short, black lines.

glass and granodiorite. Scatter in the MnO content may be due to its low values and to analytical uncertainty.

5. Fluid Inclusions

5.1. Description of the Fluid Inclusions

Our observations on polished thin sections indicate that the numerous, and apparently empty, vesicles observed by SEM by *Fujimoto et al.* [1999] in the pseudotachylyte glass are fluid inclusions. Analyses of backscattered electron (BSE) images using the public domain National Institutes of Health (NIH) Image program developed at the U.S. National Institutes of Health (NIH Image program, 1998, available at http://rsbweb.nih.gov/nih-image/) indicate that the vesicles constitute roughly 5–8% of the surface of the glass, i.e., between 0.5 and 0.8% of the volume of the melt phase assuming a regular shape and distribution of the fluid inclusions. The fluid inclusions are small, generally 1–3 μm (up to 10 μm) in their largest dimension (Figure 7). Their geometry is slightly ellipsoidal, with a shape ratio ranging from 1 to 5 or more; for larger shape ratios

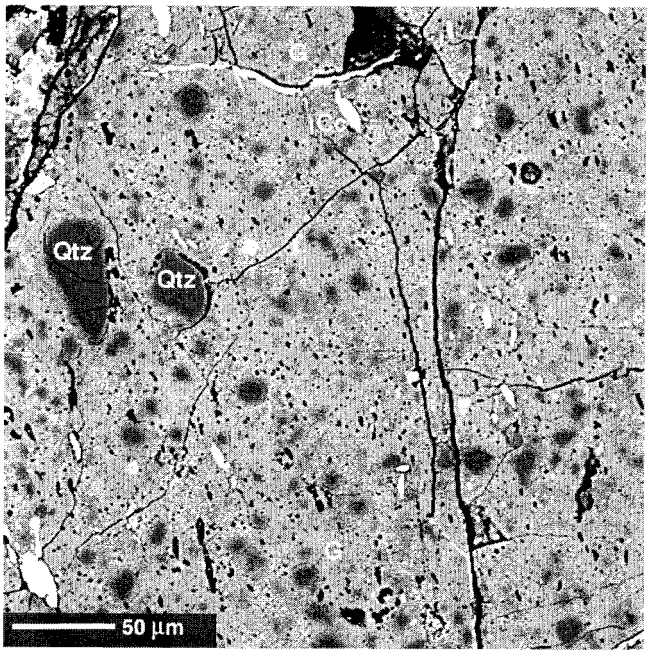

Figure 4. Heterogeneous aspect of the glass phase when observed by backscattered electron (BSE) microscopy showing calcite fragments, the blurred contours of the incompletely molten quartz fragments, and the vesicles which are elongated parallel to the layering (vertical on the microphotograph). Note the calcite-filled fracture crosscutting the layering. Qtz, quartz; Cc, calcite; G, glass.

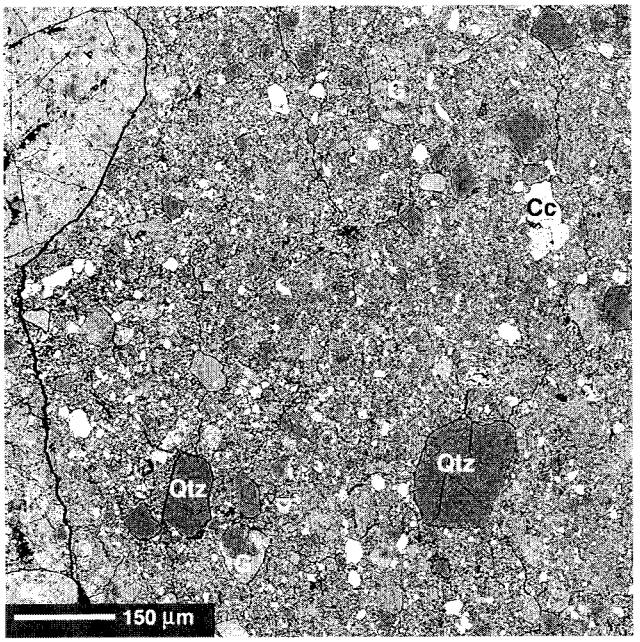

Figure 5. BSE image of ultracataclasite. The layering is vertical on this image. Note the fragments of quartz, carbonate, and pseudotachylyte glass. Qtz, quartz; Cc, calcite; G, glass.

Table 1. Chemical Compositions of the Parent Granodiorite and Pseudotachylytic Glasses in Sample 624.59[a]

		Point														
	Grano-Diorite	1	3	11	12	14	16	17	19	22	23	26	27	35	41	43
SiO_2	66.72	62.23	93.97	76.87	64.06	70.37	62.97	61.73	61.09	63.98	69.88	63.20	73.13	65.94	64.13	64.05
TiO_2	0.49	0.48	0.11	0.39	0.49	0.38	0.50	0.48	0.51	0.53	0.44	0.52	0.32	0.40	0.51	0.43
Al_2O_3	15.68	16.89	3.00	11.61	13.88	13.13	14.19	14.37	16.01	16.58	13.55	16.27	12.07	16.47	16.34	18.04
FeO	3.87	2.18	0.43	1.23	2.59	3.24	3.17	2.71	3.76	2.72	2.11	3.07	1.68	1.80	2.09	1.62
MnO	0.08	0.08	0.01	0.05	0.09	0.10	0.11	0.09	0.11	0.08	0.07	0.08	0.05	0.07	0.05	0.04
MgO	1.09	0.62	0.13	0.51	0.72	0.65	0.78	0.69	0.67	0.72	0.56	1.17	0.80	0.74	0.67	0.65
Cr_2O_3	nm	0.02	0.00	0.00	0.00	0.00	0.02	0.00	0.00	0.00	0.02	0.00	0.01	0.01	0.00	0.01
ZnO	nm	0.02	0.02	0.00	0.02	0.00	0.03	0.02	0.03	0.02	0.00	0.02	0.00	0.01	0.00	0.00
CaO	4.03	5.40	0.94	4.10	6.25	4.62	5.12	5.38	6.16	6.73	5.87	4.27	2.87	5.59	7.02	4.14
Na_2O	3.60	0.81	0.19	0.61	1.19	1.53	1.84	1.78	0.42	0.49	1.00	0.35	1.19	1.75	0.67	1.72
K_2O	2.46	1.63	0.47	0.94	1.96	1.84	2.26	2.26	1.77	1.63	1.88	1.85	1.38	1.74	1.27	1.98
P_2O_5	0.11	nm	nm	nm	nm	nm	nm	nm	nm	nm	nm	nm	nm	nm	nm	nm
LOI	1.04	nm	nm	nm	nm	nm	nm	nm	nm	nm	nm	nm	nm	nm	nm	nm
H_2O^-	0.41	nm	nm	nm	nm	nm	nm	nm	nm	nm	nm	nm	nm	nm	nm	nm
Total	99.58	90.38	99.26	96.31	91.25	95.86	90.99	89.52	90.52	93.48	95.38	90.80	93.51	94.50	92.77	92.66
SiO_2	67.99	68.86	94.67	79.82	70.21	73.41	69.20	68.96	67.49	68.44	73.27	69.60	78.20	69.78	69.13	69.12
TiO_2	0.50	0.54	0.11	0.40	0.53	0.40	0.55	0.54	0.56	0.56	0.46	0.57	0.34	0.42	0.55	0.46
Al_2O_3	15.98	18.69	3.02	12.05	15.21	13.69	15.60	16.05	17.68	17.74	14.21	17.91	12.91	17.42	17.62	19.46
FeO	3.94	2.42	0.43	1.27	2.84	3.38	3.49	3.03	4.16	2.91	2.21	3.38	1.80	1.90	2.26	1.75
MnO	0.08	0.09	0.01	0.06	0.09	0.11	0.12	0.10	0.12	0.08	0.08	0.09	0.06	0.07	0.05	0.04
MgO	1.11	0.68	0.13	0.53	0.79	0.68	0.86	0.77	0.74	0.77	0.59	1.29	0.86	0.78	0.72	0.70
Cr_2O_3	nm	0.03	0.00	0.00	0.00	0.00	0.02	0.00	0.00	0.00	0.02	0.00	0.01	0.01	0.00	0.01
ZnO	nm	0.02	0.02	0.00	0.02	0.00	0.04	0.02	0.03	0.02	0.00	0.03	0.00	0.01	0.00	0.00
CaO	4.11	5.98	0.95	4.26	6.85	4.82	5.62	6.01	6.80	7.20	6.15	4.70	3.07	5.92	7.57	4.46
Na_2O	3.67	0.90	0.19	0.64	1.31	1.59	2.02	1.99	0.47	0.52	1.04	0.39	1.27	1.85	0.73	1.85
K_2O	2.51	1.81	0.47	0.98	2.15	1.92	2.48	2.53	1.96	1.74	1.97	2.04	1.47	1.84	1.37	2.14
P_2O_5	0.11	nm	nm	nm	nm	nm	nm	nm	nm	nm	nm	nm	nm	nm	nm	nm
Total	100.00	100.00	100.00	100.00	100.00	100.00	100.00	100.00	100.00	100.00	100.00	100.00	100.00	100.00	100.00	100.00

[a]Chemical composition of the parent granodiorite [*Tanaka et al*., 1999, 2001] (with iron recalculated as FeO) and of the pseudotachylyte glasses based on electron microprobe analyses. The recalculated compositions (normalized to 100%) exclude volatiles. The point 3 analysis was not considered in the calculation of the average volatile content of the glass (91.98 ± 2.92%). nm, not measured; LOI, loss on ignition.

they often appear as gas-filled or empty. The elongation direction of the fluid inclusions is generally parallel to the pseudotachylyte layering but may also be oblique (Figure 3). They contain a two-phase H_2O-CO_2 fluid at room temperature (H_2O liquid and CO_2 liquid, with a mean 0.3 CO_2 filling ratio), except for the largest ones which are three-phase H_2O-CO_2 fluid inclusions (H_2O liquid, CO_2 liquid, and CO_2 vapor, with a 0.6 CO_2 filling ratio).

5.2. Microthermometric Study

It was not possible to observe the fluid inclusions on classical doubly polished thick wafers due to the opacity of the pseudotachylyte glass. Therefore microthermometric measurements were made on an ordinary 0.03-mm thin polished section glued to a glass plate, using a U.S. Geological Survey modified heating-cooling stage on an Olympus microscope equipped with a magnifying lens, a camera, and video monitor. The pixellization of the video image increases the image contrast, thereby facilitating the determination of the phase transition temperatures. Three phase transition temperatures have been measured (Table 2): CO_2 melting temperature (T_{mCO_2}), melting of clathrate in the presence of vapor CO_2 (T_{mclath}), and homogenization temperature of the CO_2 phase (T_{hCO_2}). It was impossible to measure the eutectic or first melting temperature of the aqueous phase because of the small size of the inclusions and the poor transparency of the sample. The bulk homogenization temperature was not measured to avoid destruction of this unique sample. The results are shown in Figure 8. CO_2 melting temperatures are relatively constant at −56.6°C, with a few lower values extending to −57.2°C. Clathrate melting temperatures range from 6.2 to 9.0°C (7.8 ± 0.7°C) and homogenization temperatures of CO_2 display a two-group distribution: The first one is concentrated around 10°C (to the liquid phase), and the second one corresponds to higher values (25 to 29°C, mostly to the vapor phase) and to the larger three-phase fluid inclusions.

5.3. Calculation of the P-V-T-X Characteristics of the Fluid

The microthermometric results are interpreted as follows: The fluid inclusions within the glass phase are almost pure CO_2 and H_2O, with some dissolved salts (4.3 ± 1.2 wt % eq NaCl). The average molal composition of the fluid (0.153 CO_2, 0.840 H_2O and 0.007 NaCl, Figure 9) has been calculated using the Q2 software by *Bakker* [1997]. Isochoric curves have been calculated from microthermometric results using the computer code by *Dubois* [1992] on the basis of a H_2O-CO_2-NaCl system [*Bowers and Helgeson*, 1983]. The two groups of CO_2 homogenization temperatures are represented by two groups of isochoric curves with steep (low $ThCO_2$) or low (high $ThCO_2$) slopes (Figure 10). Considering the mathematical applicability of *Bowers and Helgeson*'s [1983] equation, the minimum temperature of total homogenization is estimated to be 200°C.

6. Interpretation and Discussion

Because of the drill core geometry and limited volume of the sample, it was not possible to observe the fault structure over more than 5 cm. For example, pseudotachylytes in the Hiraba-

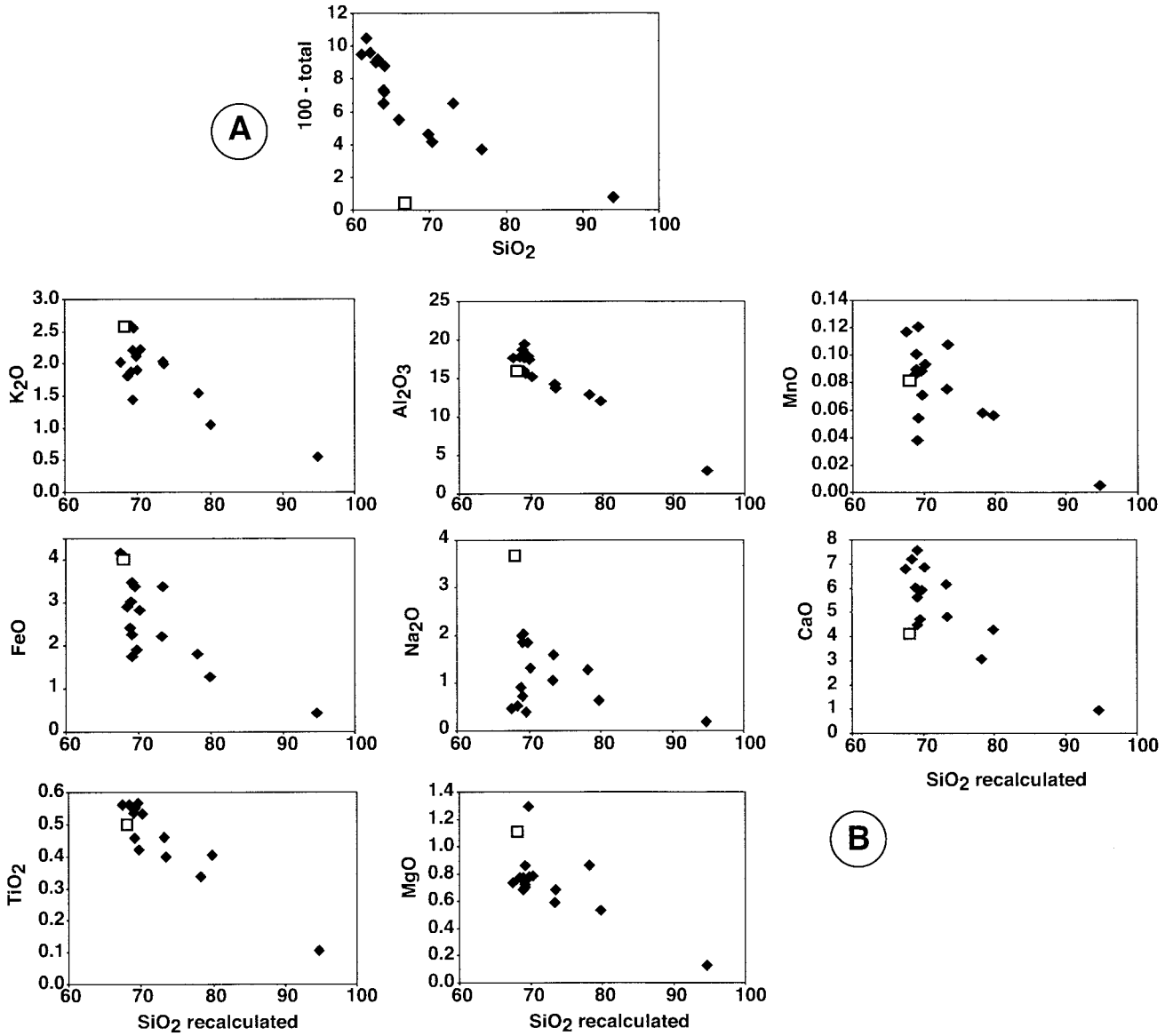

Figure 6. Composition of the pseudotachylyte glass (diamonds) and of the unaltered granodiorite (open squares). (a) Difference between 100% and total of oxides versus SiO_2 content as measured with the electron microprobe. (b) Oxide content versus SiO_2 content when recalculated (normalized to 100%) by exclusion of volatiles (see Table 2).

yashi drill hole have most frequently been observed in fault veins mostly (Figure 2), whereas pseudotachylyte injection and fault veins are often observed together in other occurrences of fault rocks [*Sibson*, 1975; *Swanson*, 1992; *Spray*, 1993; *Magloughlin*, 1992; *Lin*, 1996; *Fabbri et al*., 2000; see also *Snoke et al*., 1998, pp. 75–127]. The glassy structure of the pseudotachylyte has not been verified by electron diffraction techniques. However, simple observations, such as isotropy under crossed Nicols, homogeneous aspect on SEM, blurred contours of quartz fragments, and more specially presence of trapped, randomly distributed, dense, H_2O-CO_2 fluid inclusions which would have leaked in a granular matrix, are strongly suggestive, in our point of view, of the glassy nature of the studied Nojima fault core rock.

6.1. Composition of the Melt Phase

The maximum amount of H_2O being dissolved in a silicate melt is highly pressure dependent and slightly decreases with increasing temperature [*Holtz and Johannes*, 1994]. For example, it reaches 5 and 11 wt % at 200 and 800 MPa, respectively, in a granodioritic melt [*Naney*, 1983]. CO_2 has an identical behavior [*Holloway and Blank*, 1994]. The presence of H_2O-CO_2 fluid inclusions in the studied pseudotachylyte allows us to consider that the silicate melt was saturated in these volatiles. Therefore the high volatile content of the pseudotachylyte glass (100–92% total oxide content) as determined from the microprobe analysis and if considered as represented by H_2O and CO_2 only, may indicate a ~400 MPa (14.8 km) pressure of

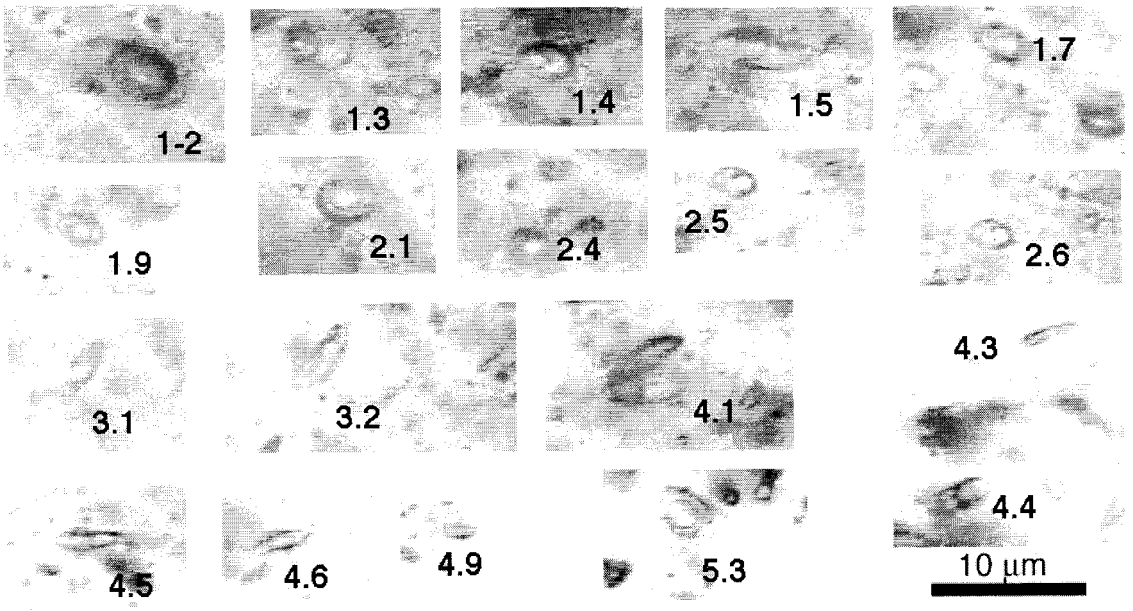

Figure 7. Microphotographs of fluid inclusions in the 624.59 sample (horizontal thin section). The numbers correspond to the fluid inclusions, as reported in Table 2. Note the three-phase CO_2-H_2O fluid inclusion (1-2), which is the largest one found in the sample.

formation by extrapolation of the Naney's experiments. This result will be discussed in section 6.3 when considering fluid inclusion data.

The high volatile content of the glass (8%) suggests that the fault rock was hydrated before frictional melting, as has already been demonstrated by *Magloughlin* [1992]. The presence of sufficient quantities of intergranular fluid within the fault and wall rock may induce a thermal pressurization event and thereby an increase in interstitial fluid pressure [*Sibson*, 1980; *Mase and Smith*, 1987; *Otsuki et al*., 1999]. Therefore intergranular fluid has been previously considered to preclude the possibility of frictional melting taking place [*Spray*, 1992]. However, considering the presence of saturated glass with fluid inclusions in the studied sample, the high volatile content of the Nojima pseudotachylytes is interpreted as resulting from incongruent melting by flash heating of a low-porosity fault rock containing H_2O-bearing minerals and carbonates. This interpretation is supported by the observation of low-porosity cataclasites within the fault zone at 619 and 622 m depth, in which altered granodiorite is compacted and cemented by zeolites and carbonates [*Boullier et al*., 1999].

Comparison of the chemical composition of the glass phase with that of the unaltered parent granodiorite, as given by *Tanaka et al*. [1999, 2001] suggests that some chemical modification of the unaltered parent granodiorite may have taken place before frictional melting. The SiO_2 content of the glass is slightly higher than that of the granodiorite and is positively correlated to the total of all oxides. This is not consistent with the observation of quartz being the last mineral to melt. One may interpret the high silica content by the heterogeneous composition of the glass phase and by the localization of the microprobe spots on, or close to, incompletely molten quartz fragments. This interpretation is supported by the dotted aspect of the glass when observed in BSE mode (Figure 4) and by the negative trend of most oxide contents (except Na_2O) relative to the SiO_2 content of the glass. It appears clearly that the glass has a similar content of Al_2O_3, TiO_2, and MnO content to that of the parent granodiorite but a higher CaO content (Figure 6). Observation of fault breccia or gouges located above the main fault plane (at 619 and 622 m depth) indicates that calcite and laumontite are common early alteration minerals in these rocks, occurring as fracture-filling minerals [*Boullier et al*., 1999; *Ohtani et al*., 2000; *Fujimoto et al*., 1999]. In the studied pseudotachylyte, some rounded remnants of calcite have also been found in the glass phase. Therefore the higher CaO content of the latter may be interpreted as resulting from the calcite alteration of the cataclasites associated with earthquakes preceding and predating the frictional melting. The Na_2O, K_2O, FeO, and MgO contents are lower in the pseudotachylyte than in the granodiorite. This may indicate that most Na-bearing (plagioclase), K-bearing (K-felspar and biotite), or Fe-Mg-bearing (biotite and amphibole) minerals were partly altered and transformed before frictional melting. This has been verified for biotite and amphiboles which are absent in the fault gouges [*Tanaka et al*., 1999, 2001] and for plagioclase clasts which were scarcely observed as fragments in the ultracataclasite associated with the studied pseudotachylytes.

The composition of the pseudotachylyte glass may also be compared with the compositional trends observed in the fault zone [*Tanaka et al*. [1999, 2001]. The fault rocks display a change in composition relative to that of the parent granodiorite, similar for some elements to that observed in the pseudotachylytes (higher SiO_2 content, lower FeO and MgO content) or different for some others (higher K_2O, lower Al_2O_3, lower CaO, unchanged Na_2O). Therefore there is no clear direct relation of the pseudotachylyte composition with that of the parent granodiorite nor with that of the fault rocks. This may be due to the complex alteration of the fault zone in space and time.

Laumontite is a common mineral filling the fractures crosscutting through the pseudotachylytes. It is not observed as

Table 2. Microthermometric Results on Fluid Inclusions in Sample 624.59[a]

Number of IF	T_{mCO_2}, °C	T_{mclath}, °C	T_{hCO_2}, °C	L or V	XCO_2, vol %
1.2	−56.6	7.3	29.0	V	0.6
1.3	−56.9	7.6	10.2	L	0.3
1.4	−56.9	8.2	10.8	L	0.3
1.5	−56.6	7.3	10.8	L	0.3
1.6	−56.6	8.2	10.3	L	0.4
1.7	−56.6	8.3	17.0	L	0.3
1.8	−56.6		7.5	L	0.4
1.9		9.0			0.3
1.10	−56.6	9.0			0.4
1.11	−56.9		27.0	V	1.0
1.12	−56.9	7.6	10.4	L	0.4
1.14	−56.8	7.9	8.2	L	0.3
2.1	−56.6	7.2	11.5	L	0.3
2.3	−56.6		11.7	L	0.4
2.4	−56.6	8.5	16.5	L	0.35
2.5	−56.6	8.2	8.6	L	0.3
2.6		8.2	9.2	L	0.3
2.7			8.0	L	0.3
2.8			12.0	L	0.3
2.9			9.5	L	0.3
3.1	−57.2	7.6	10.3	L	0.3
3.2	−57.2		11.5	L	0.3
3.3	−56.8	7.6	9.9	L	0.3
3.4	−56.8	7.6	10.3	L	0.3
3.5			10.3	L	0.3
3.6	−56.8	7.6	25.0	L	0.4
3.7	−56.6	7.6	11.0	L	0.3
4.1	−56.8	6.2	11.2	L	0.3
4.2			11.5	L	0.3
4.3	−56.6		10.0	L	0.3
4.4			10.0	L	0.3
4.5		7.0	10.4	L	0.3
4.6		8.5	11.4	L	0.3
4.7			11.2	L	0.3
4.8			9.8	L	0.3
4.9			10.0	L	0.3
4.10			10.2	L	0.3
5.1			26.0	V	0.65
5.2	−57.3	7.5	10.8	L	0.3
5.3	−56.6	6.9	14.5	L	0.3

[a]IF, fluid inclusion; T_{mCO_2}, melting temperature of CO_2; T_{mclath}, melting temperature of clathrate; T_{hCO_2}, homogenization temperature of CO_2; L, homogenization to the liquid; and V, homogenization to the vapor.

unmolten fragments. Therefore we suggest that pseudotachylytes have formed prior to the laumontite precipitation. The stability field of laumontite ranges from 130 to 200°C [*Henley and Ellis*, 1983] and corresponds to the minimum temperatures associated with the pseudotachylyte host rocks. Pseudotachylytes are also inferred to form after or during the deposition of calcite, which is observed as unmolten fragments, as well as a fracture-filling mineral. Consequently, as already stated by *Fujimoto et al*. [1999], pseudotachylytes should have formed in the very early period of the fault zone development at temperatures >200°C.

Thermal processes related to seismic rupture are probably instantaneous as slip duration is of the order of a few seconds [*Heaton*, 1990]. Therefore we assume that melting is also almost instantaneous. The melting temperature of the studied pseudotachylyte may be estimated based on the presence or absence of certain mineral phases, as was done by *Otsuki et al*. [1999] for pseudotachylytes from the same fault. Calcite and quartz, which are not completely molten, therefore indicate a higher limit of 1310°C [*Wyllie and Tuttle*, 1960] and 1726°C [*Richet et al*., 1982], respectively. The higher limit for quartz may decrease to 1100°C in the presence of water [*Kennedy et al*., 1962]. The lower limit is imposed by the liquidus of granodiorite composition at 960°C at 200 MPa [*Naney*, 1983]. As suggested by *Otsuki et al*. [1999], the folded pseudotachylyte fragments (Figure 3) incorporated within later events suggest temperature conditions high enough to plastically deform aluminosilicate glasses, i.e., 1200°C [*Bansal and Doremus*, 1986]. Given all of these data, and considering that heating processes during seismic rupture are almost instantaneous [*Swanson*, 1992] and more rapid that the melting rate of crystals, it is highly probable that melting occurred under disequilibrium conditions with possible overheating. Therefore a minimum temperature of 1200°C is a reasonable estimate for the formation of pseudotachylytes from the Nojima fault.

6.2. Thermal Behavior of the Melt Phase

The thickness of each pseudotachylyte layer is 1 mm on average, and the minimum melting temperature has been estimated to be 1200°C, as discussed previously. Using the above constraints, it is possible to calculate the cooling path of each frictional melting event and its thermal influence on the immediate

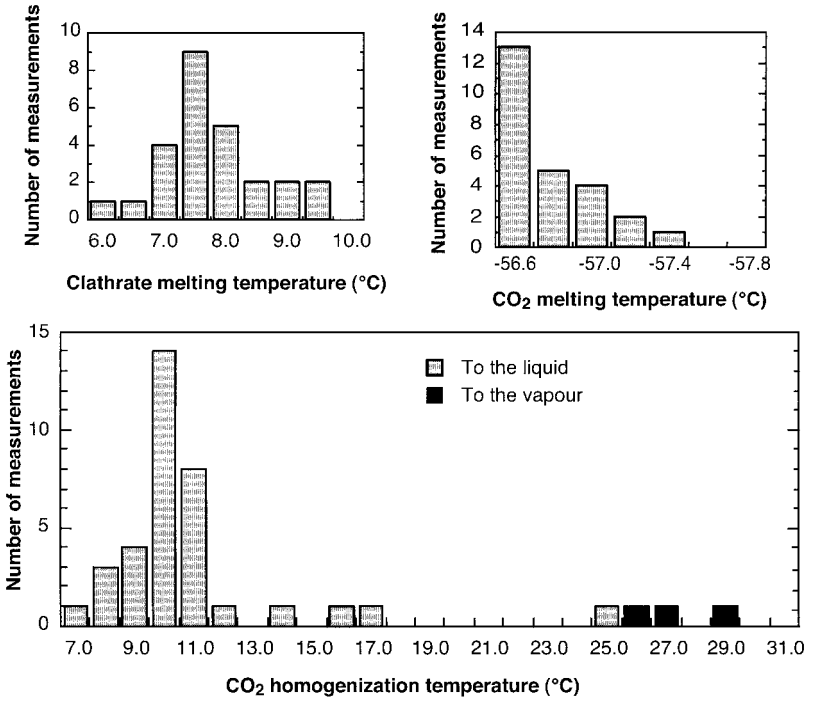

Figure 8. Microthermometric results obtained on the fluid inclusions in the 624.59 sample.

surrounding rocks using the following expression provided by *Carslaw and Jaeger* [1959, p. 54] for a semi-infinite solid:

$$T = 1/2T_0\{\mathrm{erf}[(1 - x/a)/2(\kappa t)^{1/2}] + \mathrm{erf}[(1 + x/a)/2(\kappa t)^{1/2}]\},$$

where

- x distance to center of the layer (cm);
- a half the thickness of the molten layer (cm);
- t time (s);
- T difference between temperature at a point x and temperature of surrounding rocks before melting at time t (K);
- T_0 difference between melting temperature and temperature of the surrounding rocks before melting at the point $x = 0$ (K);
- κ thermal diffusivity ($cm^2\ s^{-1}$).

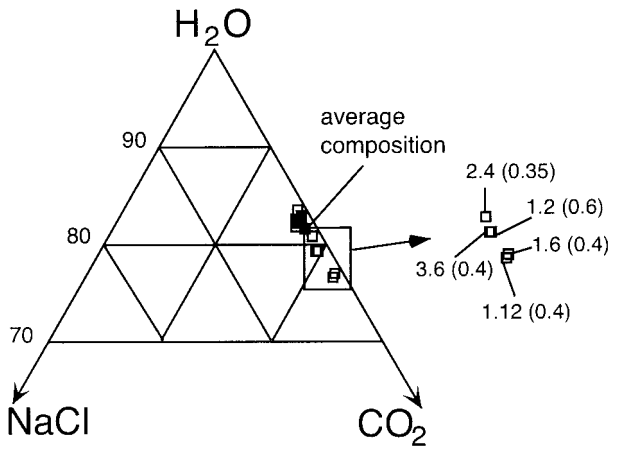

Figure 9. Ternary diagram showing the composition of the fluid inclusions in molar fractions as calculated with the Q2 software of *Bakker* [1997].

In the following calculations the temperature of the surrounding rocks is assumed to be 473 K; this corresponds to the minimum trapping temperature deduced from the fluid inclusion data (200°C) and to the upper limit of the laumontite stability field, and T_0 is equal to 1000 K (assuming a melting temperature of 1200°C). The thermal diffusivity κ has been chosen to equal 0.01 $cm^2\ s^{-1}$, as by *Dixon and Dixon* [1989].

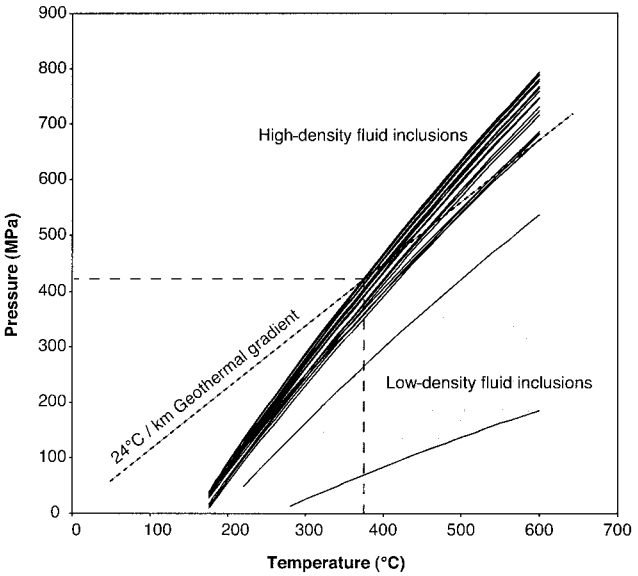

Figure 10. Isochoric curves calculated from the microthermometric results and the equation of state of *Bowers and Helgeson* [1983]. The 24°C/km geothermal gradient was measured in the GSJ drill hole [*Kitajima et al.*, 1998; *Yamaguchi et al.*, 1999]. Intersection of the isochoric curves with the geothermal gradient indicates the P-T conditions for equilibration of the fluid inclusions.

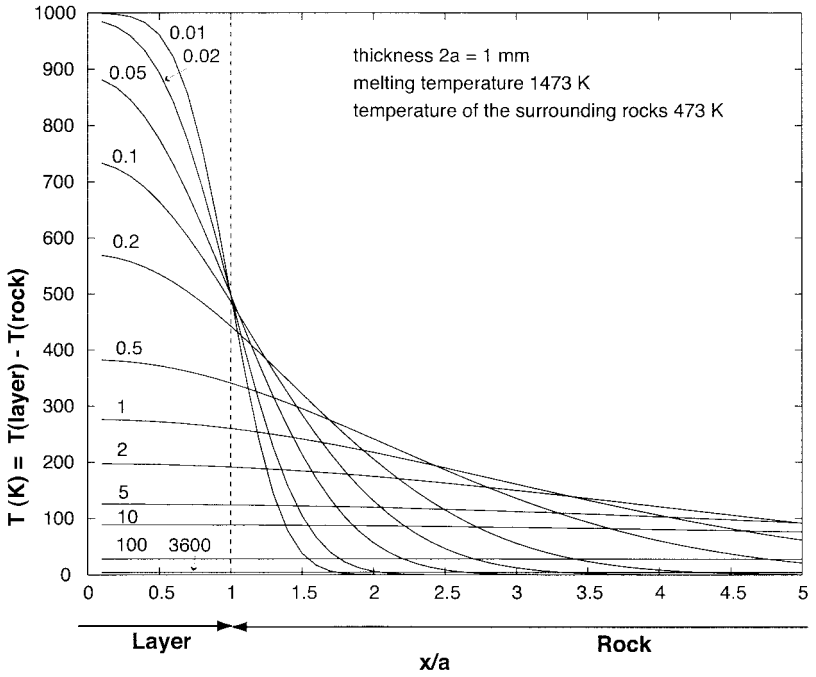

Figure 11. Cooling evolution of a 1-mm-thick molten layer [*Carslaw and Jaeger*, 1959]. T is the difference in temperature between the temperature of the molten layer and of the surrounding rocks at $t = 0$, x is the distance from the central plane of the layer, and a is the half thickness of the layer. The temperature T as a function of x/a is reported for different times t (seconds).

The results (Figure 11) indicate that at a millimeter-scale the pseudotachylyte layer cools very rapidly. The pseudotachylyte is completely solidified at $T \approx 500$ K after 0.3 s, $T = 300$ K after 1 s and $T = 100$ K after less than 10 s (Figure 11). The ambient temperature (200°C, $T = 0$) is attained after 1 hour. This implies that the viscosity of the melt decreases very quickly. Therefore enhancement of slip by melting on the fault plane should be of very short duration. It also appears from the calculation that the surrounding rocks cannot be heated by more than half the difference between the melting and ambient temperatures, i.e., 500°C in the present case. It is also possible to estimate the maximum temperature attained at a given distance from the molten layer. For example, a 400°C increase in temperature may be attained in the surrounding rock at 0.1 mm from the contact (Figure 11). This has some consequences for the interpretation of the low-density fluid inclusions, as shown below.

6.3. Significance of the Fluid Inclusions

Three types of aqueous fluids have been recognized in the core samples along the whole drill hole [*Ohtani et al*., 2000]: The first type corresponds to fluid inclusions with homogenization temperatures higher than 200°C and are related to chloritization of mafic minerals; the second corresponds to zeolite formation at <200°C; the third to carbonate precipitation (homogenization temperatures between 88 and 197°C in a calcite vein at 375.8 m depth). Consequently, as pointed out by *Ohtani et al*. [2000], all of the fluid inclusions measured in the core samples appear to correspond to higher temperatures than the present-day temperature measured at the bottom of the borehole (31°C at 746.7 m depth). Only the last two types of inclusions may be related to the fault activity. However, no H_2O-CO_2 fluid comparable to the one described in the present study has been observed.

The presence of fluid inclusions in the glass shows that the melt was saturated in H_2O and CO_2 originating from melting of H_2O-bearing minerals and carbonates, as discussed in section 6.1. The fluid inclusions have a low salinity, which is consistent with the low Na_2O content of the pseudotachylyte glass but is surprisingly low when compared to the salinity of the in situ fluids in the core samples [*Pezard et al*., 1999]. The low salinity also indicates that there was no boiling, i.e., separation of a high-salinity fluid phase from a low-salinity vapor phase, despite the very high temperature of frictional melting. This suggests that the homogeneous fluid phase was condensing in situ within the oversaturated melt during cooling.

In the Nojima pseudotachylytes, two groups of fluid inclusions appear in the density distribution. The high-density group corresponds to very close and steep isochoric curves (Figure 10). Fluid inclusions of this group are considered to have slowly equilibrated after quenching of the glass at the temperature of the surrounding rocks, which is attained <1 hour after the flash melting (Figure 11). According to this assumption they are representative of the PT conditions of the locus of pseudotachylyte formation (Figure 10) at the intersection of the isochoric curves with the geothermal gradient. The actual geothermal gradient is estimated to be 24°C/km using measurements of the thermal conductivity of the rock cores and temperature logging data in the borehole [*Kitajima et al*., 1998; *Yamaguchi et al*., 1999]. Its intersection with the isochoric curves is located at a minimum pressure of 410 MPa (i.e., 15 km) and 370°C. These pressure conditions are similar to those deduced from the volatile content of the glass (400 MPa, 14.8 km). The geothermal gradient may have been higher at the time of pseudotachylyte formation, and this would imply a lower depth estimate for the occurrence of frictional melting. For example, a 30°C/km geothermal gradient intersects the

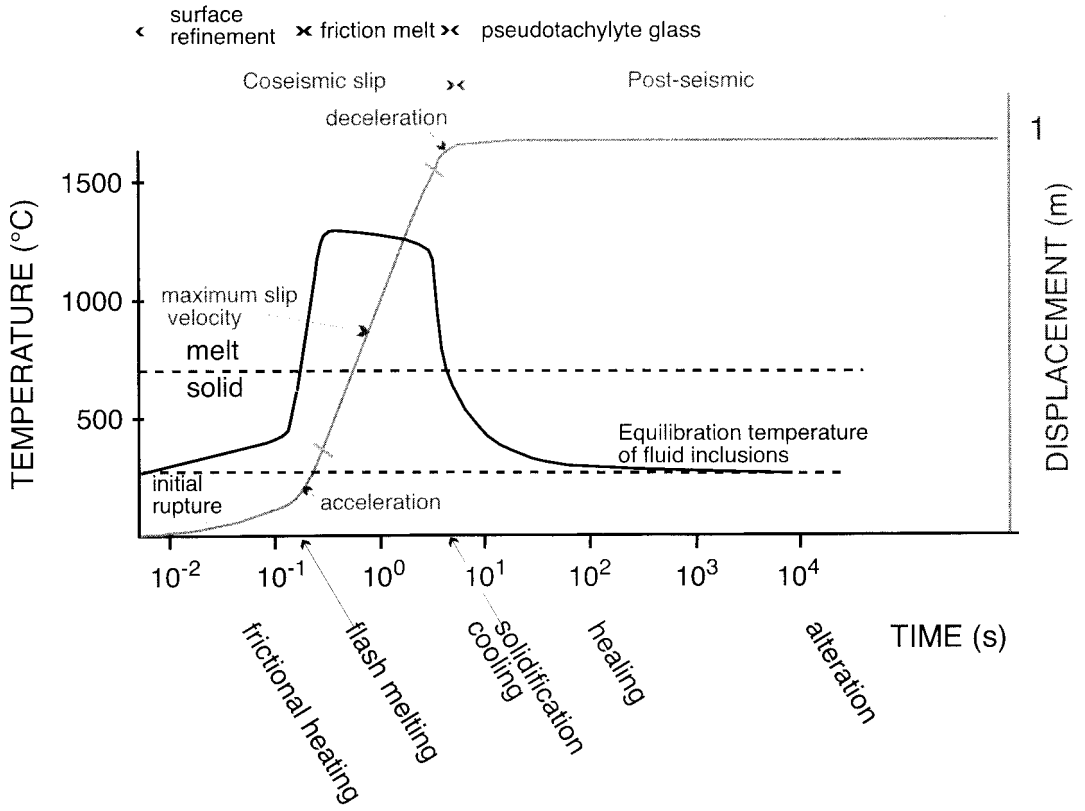

Figure 12. Schematic temperature/time and displacement/time curves modified after *Swanson* [1992] and fitted with the calculated temperature/time curves (Figure 11). This diagram shows the different stages of the seismic rupture and the very short lived thermal evolution of the Nojima pseudotachylyte-bearing fault zone.

isochores of the high-density fluid inclusions at a minimum pressure of 250 MPa (i.e., 9 km) and 280°C. Whatever the geothermal gradient, the estimates for the formation of the pseudotachylytes are much deeper than their present position (625 m) and correspond to the seismogenic zone where pseudotachylytes are thought to form [*Sibson*, 1986]. However, this would imply 9–15 km vertical displacement along a reverse fault since the formation of the pseudotachylyte, combined possibly with uplift of the whole basement. Assuming that the fault kinematics and displacement rate have remained identical since the formation of pseudotachylytes, i.e., 0.5 m/kyr [*Yokokura*, 1999], 9–15 km of reverse reverse movement on the fault would correspond to an age of 18–30 Ma. To date, there is no constraint on the age of the pseudotachylytes, except the fact that Miocene (<23.5 Ma) sediments overlay the granodioritic basement on both sides of the fault. Therefore this implies that most of the displacement should have occurred before the Miocene and that these pseudotachylytes owe their present depth (625 m) to general uplift of the region. This shows the necessity for obtaining additional information on the recent movement along the Nojima fault.

For the low-density group of fluid inclusions, we suggest a similar interpretation to that proposed by *Passchier* [1984], who describes pure CO_2 fluid inclusions, some of which are low density, in host rocks of pseudotachylytes along an uplifted low-angle major shear zone (Saint-Barthélémy massif, French Pyrénées). Following *Passchier* [1984], we postulated that these low-density fluid inclusions are due to heating and reequilibration of high-density fluid inclusions during a later seismic and pseudotachylyte-forming event. As calculated above for the Nojima pseudotachylytes, rocks located in the immediate vicinity of the molten layer are submitted to thermal stress. For example, the rise in temperature may reach 200°C at a distance of 1 mm from the molten layer contact. Therefore the fluid inclusions previously formed at these point may experience high internal overpressures (350 MPa for 200°C), sufficient to induce decrepitation or partial leaking [*Leroy*, 1979; *Pêcher*, 1981; *Pêcher and Boullier*, 1984; *Boullier et al*., 1989; *Bodnar et al*., 1989]. This interpretation is supported by the fact that only the large fluid inclusions display low density, a fact consistent with the experimental results obtained by *Leroy* [1979] and *Bodnar et al*. [1989].

6.4. Implications for Seismic Processes

In the following discussion, we use our data to infer information on seismic processes and compare this with previously proposed models. *Kanamori and Heaton* [2000] proposed a simple model of faulting in which the temperature increases with the frictional stress and the earthquake magnitude for a given thickness of the heated fault plane. Therefore the geometry and thermal budget of the Nojima fault may be used to deduce the magnitude of the seismic events during which the studied pseudotachylytes formed. To do so, we assume that the properties of the Nojima fault have not changed since the formation of the studied pseudotachylytes and that the 1995 Hyogo-ken Nanbu earthquake is a characteristic earthquake of the Nojima fault. Consequently, we use a 3–4 MPa stress calculated from the slip model [*Bouchon et al*., 1998] for the 1995 Hyogo-ken Nanbu earthquake. Using a 1-mm thickness of the fault plane, a minimum 1000°C increase in temperature,

and a 3–4 MPa initial frictional stress, we deduce a magnitude in the range 6–7 for the seismic events responsible for the Nojima pseudotachylytes on the basis of the calculations proposed by *Kanamori and Heaton* [2000, Figure 2]. Magnitude 5 values are obtained when using higher initial stresses (~10 MPa) deduced by *Spudich et al*. [1998] from striations observed on the fault plane at Hirabayashi after the 1995 Hyogo-ken Nanbu earthquake.

On the basis of the observations and possible thermal models, thermal and mechanical coupling during the seismic cycle is addressed. *Swanson* [1992] proposed a time/temperature curve for a hypothetical transient coseismic thermal spike associated with frictional melting and the production of pseudotachylytes. The calculated cooling curves for the Nojima pseudotachylytes have been incorporated in Swanson's model assuming a slip duration of a few seconds, as shown by *Irikura et al*. [1996] for the 1995 Hyogo-ken Nanbu earthquake. *Swanson* [1992] distinguishes three steps: (1) a surface refinement stage accompanied by frictional heating that results in flash melting of the fault gouge, (2) a friction melt stage, and (3) a final cooling stage. The displacement/time curve proposed by Swanson may be combined with his temperature/time curve, assuming the following criteria: acceleration of displacement occurs during frictional heating (a few tenths of seconds), maximum slip velocity during the friction melt life time (a few seconds), and deceleration during the cooling of the melt (a few seconds) where the temperature may be constrained by the cooling curves (Figure 12). Evolution of the fluid inclusions within the melt is also reported on this schematic diagram and appears to occur in a very short time (<10 s), supporting the interpretation of an equilibration at ambient conditions, i.e., during the hour following the seismic event. The most important point shown by these diagrams is the very fast healing rate of the fault plane if pseudotachylytes are formed. If, as suggested by *Kanamori and Heaton* [2000], frictional melting only occurs during large earthquakes ($M > 4.5$), the fast healing of the fault plane compared to slower healing mechanisms such as gouge compaction [*Sleep and Blanpied*, 1992] or dissolution-precipitation processes [*Gratier et al*., 1994] could be used to explain a shorter recurrence time for larger earthquakes compared to smaller ones and therefore the anomalous magnitude-frequency relationships.

7. Conclusions

Pseudotachylytes have been described in the core samples from the Hirabayashi (Awaji Island) borehole that was drilled though the Nojima fault 1 year after the 1995 Hyogo-ken Nanbu earthquake. Pseudotachylytes formed by frictional melting were not formed at their present level (624.59 m depth) but at much deeper levels. Fluid inclusions have been described for the first time in the glass phase within these pseudotachylytes. The study of textures, composition of the glass phase and unmolten fragments, and fluid inclusions, combined with an estimated cooling rate of the frictional melt lead to the following conclusions:

1. Frictional melting and pseudotachylyte formation occurred in an already altered, calcite-bearing and hydrated fault zone, as deduced by the high volatile content of the glass phase.

2. Fluid inclusions within the glass are filled by a dense low-salinity CO_2-H_2O fluid, which corresponds to steep isochores. The intersection of these isochores with the 24°C/km present regional geothermal gradient indicates a 15-km minimum depth of formation for these pseudotachylytes, corresponding to the bottom of the seismogenic zone. This depth is also consistent with the $8.0 \pm 3.0\%$ volatile content of the glass phase and suggests that pseudotachylytes are pre-Miocene and that an important regional uplift event occurred before Miocene time. Better knowledge of the geodynamic evolution of the Nojima fault and a determination of the age of the pseudotachylyte are now necessary to understand the complex history of this fault.

3. Thermal evolution of the glass and therefore of the fluid inclusions was very fast and did not last more than a few seconds. This means that the related seismic processes, such as deceleration of displacement and healing of the fault, were also very rapid.

4. The geometry and thermal budget of the millimeter-thick pseudotachylytes allow for estimated magnitudes in the range 6 to 7 with respect to seismic events responsible for their formation.

Acknowledgments. The authors thank all the participants of the Tsukuba workshop and, in particular, K. Otsuki for discussions during the meeting. In addition, thanks are extended to M. Bouchon and R. J. Archuleta for fruitful discussions on seismology; M. Yamano and A. Tanaka for the discussion on the temperature gradient; B. Ildefonse, J.-P. Gratier, and P. Pezard for every day support and discussions; C. Nevado for making the delicate thin sections, S. Pairis for SEM observations; J.-M. Montel and P. Barbey for petrologic interpretations; O. Fabbri for discussion on thin sections of the Japanese pseudotachylytes; P. Favreau and C. Voisin for their help with the thermal modeling; J. Magloughlin for careful review of the manuscript; and R. Hellmann for improvement of the English. This work was financially supported by the CNRS and ANDRA through the GdR FORPRO (research action 99.III) and corresponds to GDR FORPRO contribution 2001/02 A.

References

Awata, Y., and K. Mizuno, Strip map of the surface fault ruptures associated with the 1995 Hyogo-ken Nanbu earthquake, central Japan—The Nojima, Ogura and Nadagawa earthquake faults, Geol. Surv. of Jpn., Tsukuba, 1997.

Bakker, R. J., Clathrates: Computer programs to calculate fluid inclusion V-X properties using clathrate melting temperatures, *Comput. Geosci*., *23*, 1–18, 1997.

Bansal, N. P., and R. H. Doremus, *Handbook of Glass Properties*, Academic, San Diego, Calif., 1986.

Bodnar, R. J., P. R. Binns, and D. L. Hall, Synthetic fluid inclusions-VI. Quantitative evaluation of the decrepitation behaviour of fluid inclusions in quartz at one atmosphere confining pressure, *J. Metamorph. Geol*., *7*, 229–242, 1989.

Bouchon, M., H. Sekiguchi, K. Irikura, and T. Iwata, Some characteristics of the stress field of the 1995 Hyogo-ken Nanbu (Kobe) earthquake, *J. Geophys. Res*., *103*, 24,271–24,282, 1998.

Boullier, A. M., G. Michot, A. Pêcher, and O. Barrès, Diffusion and/or plastic deformation around fluid inclusions in synthetic quartz: New investigations, in *Fluid Movements—Element Transport and the Composition of the Deep Crust*, edited by D. Bridgwater, pp. 345–360, Kluwer Acad., Norwell, Mass., 1989.

Boullier, A. M., B. Ildefonse, J. P. Gratier, K. Fujimoto, T. Ohtani, and H. Ito, Deformation textures and mechanisms in the granodiorite from the Nojima Hirabayashi borehole, in *International Workshop of the Nojima Fault Core and Borehole Data Analysis*, edited by H. Ito et al., pp. 111–117, Geol. Surv. of Jpn., Tsukuba, 1999.

Bowers, T. S., and H. C. Helgeson, Calculation of the thermodynamic and geochemical consequences of nonideal mixing in the system H_2O-CO_2-NaCl on phase relations in geological systems: Equation of state for H_2O-CO_2-NaCl fluids at high pressures and temperatures, *Geochim. Cosmochim. Acta*, *47*, 1247–1275, 1983.

Carslaw, H. S., and J. C. Jaeger, *Conduction of Heat in Solids*, 510 pp., Oxford Univ. Press, New York, 1959.

Dixon, J. E., and T. H. Dixon, Vesicles, amygdales and similar structures in fault-generated pseudotachylytes—Comment, *Lithos*, *23*, 225–227, 1989.

Dubois, M., Fluides crustaux: Approche expérimentale et analytique, 1, Détermination du solvus des systèmes H_2O-MCl (M=Li, K, Rb, Cs) et, 2, Caractérisation et dynamique des fluides des dômes thermiques sur l'exemple du diapir vellave (S-E Massif central français), Doctorat d'université thesis, Inst. Natl. Polytech. de Lorraine, Nancy, France, 1992.

Fabbri, O., A. Lin, and H. Tokushige, Coeval formation of cataclasite and pseudotachylyte in a Miocene forearc granodiorite, southern Kyushu, Japan, *J. Struct. Geol*., *22*, 1015–1025, 2000.

Fujimoto, K., H. Tanaka, N. Tomida, T. Ohtani, and H. Ito, Characterization of fault gouge from GSJ Hirabayashi core samples and implications for the activity of the Nojima fault, in *International Workshop of the Nojima Fault Core and Borehole Data Analysis*, edited by H. Ito et al., pp. 103–109, Geol. Surv. of Jpn., Tsukuba, 1999.

Gratier, J. P., T. Chen, and R. Hellman, Pressure solution as a mechanism for crack sealing around faults, in *Proceedings of Workshop LXIII: The Mechanical Involvement of Fluids in Faulting*, pp. 279–300, U.S. Geol. Surv., Menlo Park, Calif., 1994.

Heaton, T. H., Evidence for and implications of self-healing pulses of slip in earthquake rupture, *Phys. Earth Planet. Inter*., *64*, 1–20, 1990.

Henley, R. W., and A. J. Ellis, Geothermal systems, ancient and modern: A geochemical review, *Earth Sci. Rev*., *19*, 1–50, 1983.

Holloway, J. R., and J. G. Blank, Application of experimental results to C-O-H species in natural melts, in *Volatiles in Magmas*, edited by M. R. Carroll and J. R. Holloway, pp. 187–230, Mineral. Soc. of Am., Washington, D. C., 1994.

Holtz, F., and W. Johannes, Maximum and minimum water contents of granitic melts: Implications for chemical and physical properties of ascending magmas, *Lithos*, *32*, 149–159, 1994.

Irikura, K., T. Iwata, H. Sekiguchi, A. Pitarka, and K. Kamae, Lesson from the 1995 Hyogo-ken Nanbu earthquake: Why were such destructive motions generated to buildings?, *J. Nat. Disaster Sci*., *17*(2), 99–127, 1996.

Ito, H., T. Kuwahara, O. Miyazaki, T. Kiguchi, K. Fujimoto, T. Ohtani, H. Tanaka, S. Higuchi, S. Agar, A. Brie, and H. Yamamoto, Structure and physical properties of the Nojima fault (in Japanese with English abstract), *Geophys. Explor*., *49*, 522–535, 1996.

Ito, H., Y. Kuwahara, T. Kiguchi, K. Fujimoto, and T. Ohtani, Outline of the Nojima fault drilling by GSJ: Structure, physical properties and permeability structure from borehole measurements in GSJ borehole crossing the Nojima fault, Japan, in *International Workshop of the Nojima Fault Core and Borehole Data Analysis*, edited by H. Ito et al., pp. 71–79, Geol. Surv. of Jpn., Tsukuba, 1999.

Kanamori, H., and T. H. Heaton, Microscopic and macroscopic physics of earthquakes, in *GeoComplexity and the Physics of Earthquakes*, *Geophys. Monogr. Ser*., vol. 120, edited by J. Rundle, D. L. Turcotte, and W. Klein, pp. 147–163, AGU, Washington, D. C., 2000.

Kennedy, G. C., G. J. Wasserburg, H. C. Heard, and R. C. Newton, The upper three phase region in the system SiO_2-H_2O, *Am. J. Sci*., *260*, 501–521, 1962.

Kitajima, T., Y. Kobayashi, R. Ikeda, Y. Iio, and K. Omura, Terrestrial heat flow in Nojima-Hirabayashi, Awaji Island (in Japanese), *Chikyu Mon*., *21*, 108–113, 1998.

Leroy, J., Contribution à l'étalonnage de la pression interne des inclusions fluides lors de leur décrépitation, *Bull. Minéral*., *102*, 584–593, 1979.

Lin, A., Injection veins of crushing-originated pseudotachylyte and fault gouge formed during seismic faulting, *Eng. Geol*., *43*, 213–224, 1996.

Magloughlin, J. F., Microstructural and chemical changes associated with cataclasis and frictional melting at shallow crustal levels: The cataclasite-pseudotachylyte connection, *Tectonophysics*, *204*, 243–260, 1992.

Magloughlin, J. F., and J. G. Spray, Frictional melting processes and products in geological materials: Introduction and discussion, *Tectonophysics*, *204*, 197–204, 1992.

Mase, C. W., and L. Smith, Effects of frictional heating on the thermal, hydrologic and mechanical response of a fault, *J. Geophys. Res*., *92*, 6249–6272, 1987.

Naney, M. T., Phase equilibria of rock-forming ferromagnesian silicates in granitic systems, *Am. J. Sci*., *283*, 993–1033, 1983.

Ohtani, T., K. Fujimoto, H. Ito, H. Tanaka, N. Tomida, and T. Higuchi, Fault rocks and past to recent fluid characteristics from the borehole survey of the Nojima fault ruptured in the 1995 Kobe earthquake, southwest Japan, *J. Geophys. Res*., *105*, 16,161–16,171, 2000.

Otsuki, K., N. Monzawa, and T. Nagase, Thermal pressurization, fluidization and melting of fault gouge during seismic slip recorded in the rock from Nojima fault, in *International Workshop of the Nojima Fault Core and Borehole Data Analysis*, edited by H. Ito et al., pp. 43–50, Geol. Surv. of Jpn., Tsukuba, 1999.

Passchier, C. W., Fluid inclusions associated with the generation of pseudotachylyte and ultramylonite in the French Pyrenees, *Bull. Minéral*., *107*, 307–315, 1984.

Pêcher, A., Experimental decrepitation and reequilibration of fluid inclusions in synthetic quartz, *Tectonophysics*, *78*, 567–584, 1981.

Pêcher, A., and A. M. Boullier, Evolution à pression et température élevées d'inclusions fluides dans un quartz synthétique, *Bull. Minéral*., *107*, 139–153, 1984.

Pezard, P., H. Ito, D. Hermitte, and A. Revil, Electrical properties and alteration of granodiorites from the GSJ Hirabayashi hole, Japan, in *International Workshop of the Nojima Fault Core and Borehole Data Analysis*, edited by H. Ito et al., pp. 255–262, Geol. Surv. of Jpn., Tsukuba, 1999.

Reed, S. J. B., *Electron Microprobe Analysis and Scanning Electron Microscopy in Geology*, 215 pp., Cambridge Univ. Press, New York, 1996.

Richet, P., Y. Bottinga, L. Denielou, J. P. Petitet, and C. Tequi, Thermodynamic properties of quartz, cristobalite and amorphous SiO_2: Drop calorimetry measurements between 1000 and 1800 K and a review from 0 to 2000 K, *Geochim. Cosmochim. Acta*, *46*, 2639–2658, 1982.

Sibson, R. H., Generation of pseudotachylyte by ancient seismic faulting, *Geophys. J. R. Astron. Soc*., *43*, 775–794, 1975.

Sibson, R. H., Power dissipation and stress levels on faults in the upper crust, *J. Geophys. Res*., *85*, 6239–6247, 1980.

Sibson, R. H., Earthquakes and rock deformation in crustal fault zones, *Annu. Rev. Earth Planet. Sci*., *14*, 149–175, 1986.

Sleep, N., and M. Blanpied, Creep, compaction and weak rheology of major faults, *Nature*, *359*, 687–692, 1992.

Snoke, A. W., J. Tullis, and V. R. Todd, *Fault-Related Rocks: A Photographic Atlas*, Princeton Univ. Press, Princeton, N. J., 1998.

Spray, J. G., A physical basis for the frictional melting of some rock-forming minerals, *Tectonophysics*, *204*, 205–221, 1992.

Spray, J. G., Viscosity determinations of some frictionally generated silicate melts: Implications for fault zone rheology at high strain rates, *J. Geophys. Res*., *98*, 8053–8068, 1993.

Spudich, P., M. Guateri, K. Otsuki, and J. Minagawa, Use of fault striations and dislocation models to infer tectonic shear stress during the 1995 Hyogo-ken Nanbu (Kobe) earthquake, *Bull. Seismol. Soc. Am*., *88*, 413–427, 1998.

Swanson, M. T., Fault structure, wear mechanisms and rupture processes in pseudotachylyte generation, *Tectonophysics*, *204*, 223–242, 1992.

Tanaka, H., N. Tomida, N. Sekiya, Y. Tsukiyama, K. Fujimoto, T. Ohtani, and H. Ito, Distribution, deformation and alteration of fault rocks along the GSJ core penetrating the Nojima fault, Awaji Island, southwest Japan, in *International Workshop of the Nojima Fault Core and Borehole Data Analysis*, edited by H. Ito et al., pp. 81–101, Geol. Surv. of Jpn., Tsukuba, 1999.

Tanaka, H., K. Fujimoto, T. Ohtani, and H. Ito, Structural and chemical characterization of shear zones in the freshly activated Nojima fault, Awaji Island, southwest Japan, *J. Geophys. Res*., *106*, 8789–8810, 2001.

Wyllie, P. J., and O. F. Tuttle, The system CaO-CO_2-H_2O and the origin of carbonatites, *J. Petrol*., *1*, 1–46, 1960.

Yamaguchi, T., M. Yamano, T. Nagao, and S. Goto, Temperature monitoring in a borehole drilled into the Nojima fault and radioactive heat production of core samples, in *International Workshop of the Nojima Fault Core and Borehole Data Analysis*, edited by H. Ito et al., pp. 277–282, Geol. Surv. of Jpn., Tsukuba, 1999.

Yokokura, T., Seismic investigation of an active fault off Kobe: another disaster in the making?, *Leading Edge*, *18*(12), 1417–1421, 1999.

A.-M. Boullier, LGIT, CNRS, UMR 5559, Université Joseph Fourier, BP 53, F-38041 Grenoble, France. (Anne-Marie.Boullier@obs.ujf-grenoble.fr)

M. Dubois, Sédimetologie et Géodynamique, FRE 2255, Université des Sciences et Techniques de Lille, F-59655 Villeneuve d'Ascq Cedex, France. (Michel.Dubois@univ-lille1.fr)

K. Fujimoto, H. Ito, and T. Ohtani, Geological Survey of Japan, AIST, Central 7, 1-1-1, Higashi, Tsukuba, Ibaraki 305-8567, Japan. (k-fujimoto@aist.go.jp; jisao.itou@aist.go.jp; tomo-ohtani@aist.go.jp)

(Received November 3, 2000; revised May 31, 2001;
accepted June 9, 2001.)